RSC Advances

ROYAL SOCIETY OF CHEMISTRY

www.rsc.org/advances

Hydrophilic modification of polyvinyl chloride hollow fiber membranes by silica with a weak in situ sol-gel method

Hai-Peng Xu, Yan-Hong Yu, Wan-Zhong Lang*, Xi Yan, Ya-Jun Guo

The Education Ministry key Laboratory of Resource Chemistry and Shanghai Key Laboratory of Rare Earth Functional Materials, Department of Chemistry and Chemical Engineering, Shanghai Normal University, 100 Guilin Road, Shanghai 200234, China

* Corresponding author. wzlang@shnu.edu.cn (W.Z. Lang); Tel: +86-21-64321951; Fax: +86-21-64321951.

Abstract

A weak in situ sol-gel method is proposed to the hydrophilic modification of polyvinyl chloride (PVC) hollow fiber membranes by silica, which is generated by the soft hydrolysis of tetraethoxysilane (TEOS) in deionized water bath. The silica is uniformly distributed on the membrane surface. The sponge-like structure of the modified PVC membranes becomes thicker with the addition of TEOS. The surface hydrophilicity of the membranes gradually increases due to the introduction of silica. The hydraulic permeability increases from 34.8 $L \cdot M^{-2} \cdot H^{-1} \cdot bar^{-1}$ to 89.1 $L \cdot M^{-2} \cdot H^{-1} \cdot bar^{-1}$, and then decreases to 45.3 $L \cdot M^{-2} \cdot H^{-1} \cdot bar^{-1}$ for the membranes of M0(1,3,5)E50 with the addition of TEOS from 0 to 5 wt.% in the dopes when 50 wt.% ethanol aqueous solution is used as bore liquid. The similar tendency is found for the membranes M0(1,3,5)D95 with 95 wt.% DMAc aqueous solution as bore liquid. The anti-fouling experiments illustrate that the membranes with the addition of TEOS show higher anti-fouling ability. Moreover, the mechanical properties of the PVC membranes are also enhanced with the introduction of silica. This work demonstrates that the PVC inorganic-organic composite hollow fiber membranes are prepared by a weak in situ sol-gel method, which avoids using corrosive substances during membrane preparation.

Key Words: Polyvinyl chloride; Ultrafiltration; Hollow fiber membrane; Sol-gel; Silica

1. Introduction

Polyvinyl chloride(PVC) ultrafiltraion membranes have been widely applied in drinking water production, membrane bioreactor(MBR) and other water treatments due to low cost, good separation performances as well as mechanical properties [1-13]. However, the traditional PVC membranes are still greatly limited by membrane fouling for its hydrophobic property which reduces permeability, needs frequent chemical cleaning and increases operation cost. The foulants on membrane surface and in pores shorten the membrane life [6]. Currently, many methods were employed to improve the properties of polymeric membranes in term of antifouling ability, hydrophilicity, and mechanical properties etc. Among these methods, blending modification is an facile and efficient method which makes preparation and modification be completed in a single step[14]. The introduced additives include hydrophilic polymers such as polymethyl methacrylate(PMMA)[2], polyethylene glycol(PEG)[15], perfluorosulfonic acid (PFSA)[16] and polyvinylpyrrolidone (PVP)[17] etc. and inorganic nano-fillers such as carbon nanotubes(CNTs)[18], TiO_2[19], ZnO[20], SiO_2[21]and so on. However, blending method is always difficult to avoid the agglomeration of nano-particles, especially in those cases with high particle content. The agglomeration causes large defects and limits the improvement of membrane performances[22,23]. Recently the sol–gel method, as a classic way for the nano-particle fabrication of silica, was employed to prepare organic–inorganic hybrid membranes[24-30]. This method can not only introduce nano-fillers into membrane matrix, but also effectively prevent the aggregation of them. Liang et al.[25] prepared poly(vinylidene fluoride) (PVDF)/silica (SiO_2) hybrid membranes by thermally induced phase separation (TIPS). The surface hydrophilicity, pure water flux and mechanical properties were obviously improved with the formation of SiO_2 particles in the hybrid membranes. Yu et al. [30] prepared PVDF/SiO_2 organic–inorganic composite hollow fiber ultrafiltration (UF) membranes via a tetraethoxysilane (TEOS) sol–gel process combined with wet-spinning method. The in situ formed SiO_2 fillers

were homogenously dispersed in PVDF matrix and apparently improved the mechanical property, thermal stability, permeation and antifouling performance of the hybrid membranes.

However, it is worth noting that all these works introduced acid solution or alkali aqueous solution as coagulation liquid to induce the hydrolysis and polycondensation of TEOS. After membrane preparation, the abundant acid or alkali waste water would be generated. This is unacceptable for green chemical process. Additionally, adding acid or alkali in coagulation liquid also increases the cost of membrane production. In this work, the PVC membranes were modified by silica with a weak in situ sol-gel method via the soft hydrolysis reaction of TEOS in water. The effects of TEOS on the membrane properties such as morphology, hydrophilicity, permeability and anti-fouling ability, pore size and mechanical properties were discussed in detail.

2. Experimental

2.1. Materials

PVC with the polymerization degree of 1300 in powder form was purchased by Shanghai Chlor Alkali Chem. Co., Ltd. (China). TEOS, glycerol and N, N-dimethylacetamide(DMAc) were purchased from Shanghai Chemical Agent Company (PR China). PEGs with different molecular weights were purchased from Sigma-Aldrich (Shanghai) Trading Co. Ltd (China). Bovine serum albumin (BSA, M_W=67,000) was purchased from Shanghai Bio Co. Ltd. (China).

2.2. Preparation of PVC hollow fiber membranes

The PVC hollow fiber membranes were spun at 25±1°C with wet spinning method. First, PVC powder was first dried in an oven at 70 °C. Then, 15 wt.% PVC, 6 wt.% glycerol and different amounts of TEOS were dissolved into DMAc solvent by mechanical stirring at 70 °C for 24 h to get homogenous dope solutions. The dope solutions were kept in a tank over night for degassing before spinning.

Table 1 The detailed preparation conditions of PVC hollow fiber membranes.

Membrane no.	Dope composition (PVC/TEOS/glycerol/DMAc)	Bore composition (wt.%)	Dope viscosity (mPa·s)
M0E50	15/0/6/79	Ethanol/water:50/50	4440
M0D95		DMAc/water:95/5	
M1E50	15/1/6/78	Ethanol/water:50/50	5080
M1D95		DMAc/water:95/5	
M3E50	15/3/6/76	Ethanol/water:50/50	5760
M3D95		DMAc/water:95/5	
M5E50	15/5/6/74	Ethanol/water:50/50	6420
M5D95		DMAc/water:95/5	

The dope solution and bore liquid passed through a spinneret under the pressure of N_2 and constant-flow pump, respectively. External coagulation bath was tap water at 25±1°C and bore liquid was 50wt.% ethanol aqueous solution or 95 wt.% DMAc aqueous solution. The fabricated PVC fibers were immersed into water for at least 24 h to further induce the hydrolysis of TEOS and remove residual solvents. Then, the fibers were kept in 50 wt.% glycerol aqueous solution for 24 h to avoid the collapse of porous structure and stored in a sealed space at room temperature for testing. The viscosity of dopes was tested by a rotational viscometer. The detailed preparation parameters were listed in Table 1.

2.3. Membrane characterizations

2.3.1. Characterizations of silica on membrane surface

To verify the hydrolysis of TEOS, energy dispersive spectroscopy (EDS) was used to detect the silicon element and oxygen element of membrane surface M5E50 with the highest TEOS concentration. The FTIR

spectra of membrane M5E50 were measured using a Fourier-transform infrared spectrometer (FTIR-ATR ElectronCorp Nicolet 380) from 800 to 2000 cm^{-1}. Meanwhile, M5E50 membrane samples were put into water with vigorous stirring to test the leaching of silicon element.

2.3.2. Morphology

The morphologies of all PVC membranes were examined by a field emission scanning electron microscopy (FESEM) (Hitachi S-4800, Japan). The samples were coated with gold under vacuum before testing.

The outer surfaces of membranes M0(1,3,5)E50 were detected by an atomic-force microscopy (AFM, BioScope TM, USA) using tapping mode. The prepared membranes were placed in a glass substrate and the surface was scanned in a size of 2 μm×2 μm with a scanning speed of 2 Hz. The average roughness (R_a), roughness (R_q), surface skewness (R_{sk}) and surface kurtosis (R_{ku}) values were calculated by equals [31,32].

2.3.3. Dynamic contact angle

A dynamic contact angle experiment was conducted to detect the surface hydrophilicity of PVC hollow fiber membranes by a contact angle analyzer (KRÜSS DSA30, German).

2.3.4. Permeation and rejection performances

The hydraulic permeabilities (J_w) of PVC hollow fiber membranes were measured at 1.0 bar with deionized water at 25 ± 1 °C. The ultrafiltration system was self-prepared and revealed in the previous reports[33,34]. All modules were pre-pressured at 2.0 bar about 30 min before testing. Then, the J_w was calculated according to

$$J_w = V / (A \cdot t) \qquad \text{Eq.(1)}$$

where V is the volume of pure water volume(L), A is the effective membrane area (m^2), t is the running time (h).

The rejections of PVC hollow fiber membranes were conducted by 500 ppm BSA aqueous solution at 1.0 bar. The BSA concentrations of permeate and feed solutions were determined by an UV-spectrophotometer (UV3600 Shimadzu, Japan) at 280 nm. The rejection of BSA was defined as

$$R = (1 - \frac{C_P}{C_F}) \times 100 \quad \text{Eq.(2)}$$

where C_P and C_F are the permeate and feed concentrations respectively.

To elucidate the anti-fouling ability of PVC hollow fiber membranes, cyclic filtration tests were performed on M0(1,3,5)E50 which included thrice fouling and twice washing. The fouled modules were washed with 500 ppm NaClO aqueous solution at 25 °C for 30 min[35,36]. The modules were rinsed with DI water, and then the J_w was tested again. The relative flux reduction (RFR) and the flux recovery ratio (R_J) were evaluated by

$$RFR(\%) = (1 - J_P / J_w) \times 100 \quad \text{Eq.(3)}$$

$$R_J(\%) = J_R / J_w \times 100 \quad \text{Eq.(4)}$$

where J_p is BSA aqueous solution flux after each fouling process and J_R is re-measured water flux of the membranes after regeneration in each cycle.

Series of PEG ultrafiltration experiments were conducted to evaluate the mean pore size ($\overline{d}_p$) and MWCO of PVC hollow fiber membranes[37,38]. The concentration of PEG solutions were kept at 200 ppm. The detailed equals were mentioned before[39-41].

2.4.5. Mechanical properties

The mechanical properties of PVC hollow fiber membranes were evaluated by a material test machine (QJ210A, Shanghai Qingji Instrumentation Sci. & Tech. Co., Ltd, Shanghai, China). All samples were tested at last five times with the stretching rate at 50 mm/min.

3. Results and discussion

3.1. Characterization of silica on membrane surface

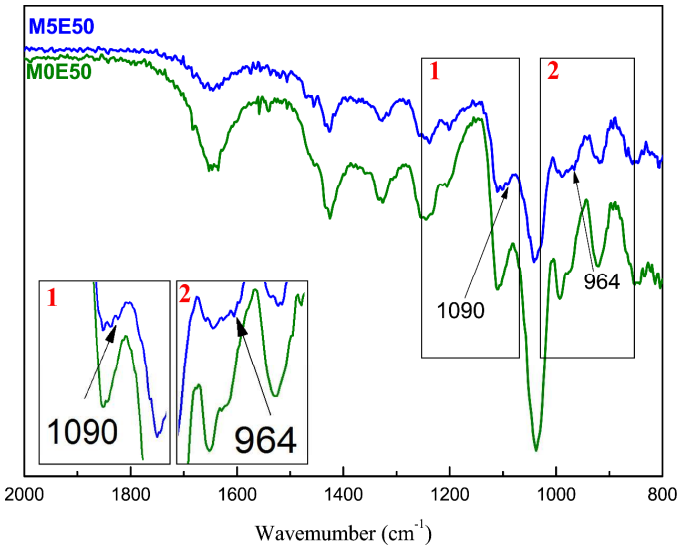

Fig.1 The FTIR-ATR spectra of membrane M5E50

Fig.1 shows the FTIR spectra of membranes M0E50 and M5E50. In comparison with M0E50, M5E50 shows two new weak peaks at 964 cm^{-1} and 1090 cm^{-1} which are referred to Si-OH and Si-O-Si bonds respectively[25,30]. EDS test was further used to detect the silica on outer surface of membrane M5E50 and the element contents are obtained. According to calculations from the results, there exists 0.76±0.10 wt.% silicon element and 10.40±2.40 wt.% oxygen element on membrane surface of M5E50. The EDS maps are shown in Fig.2. This verifies that the added TEOS has been hydrolyzed to silica after immersing into water. From the distribution (Fig.2) of silicon element and oxygen element, it can be seen that silica fillers are introduced and uniformly distributed on the membrane surfaces. After vigorous stirring for 24h, there still exists 0.65±0.10 wt.% silicon element. It means that the interaction force between silicon dioxide and membrane matrix is well.

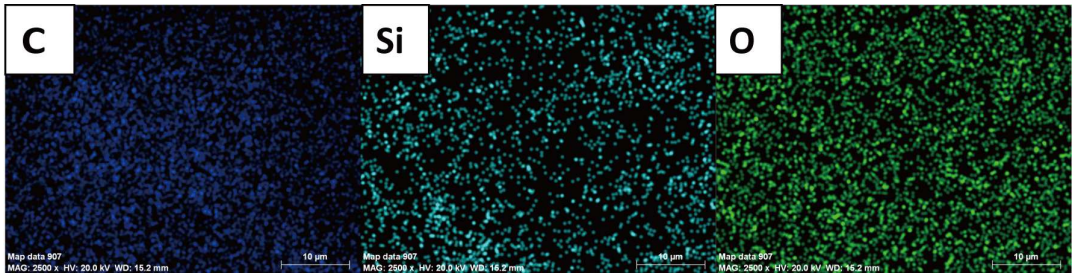

Fig.2 The EDS maps of the outer membrane surface of M5E50

3.2. Morphology

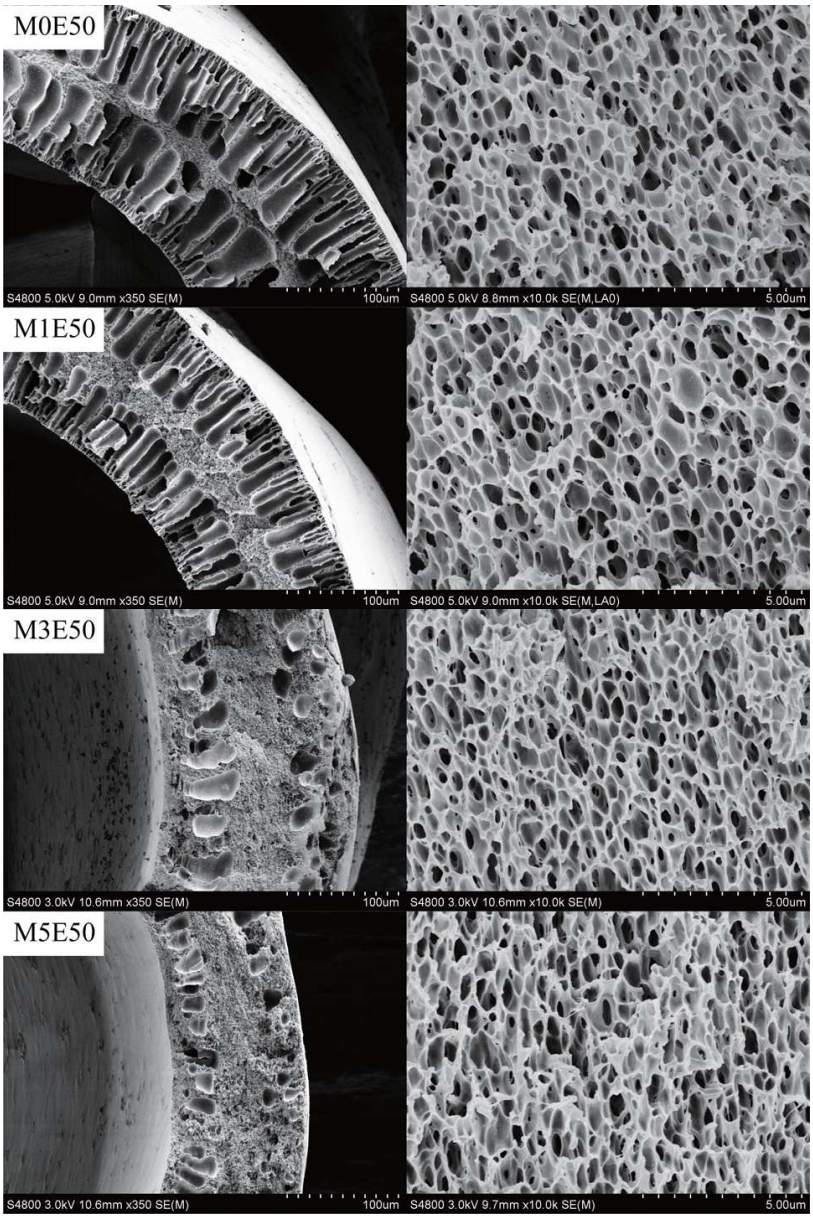

(A)

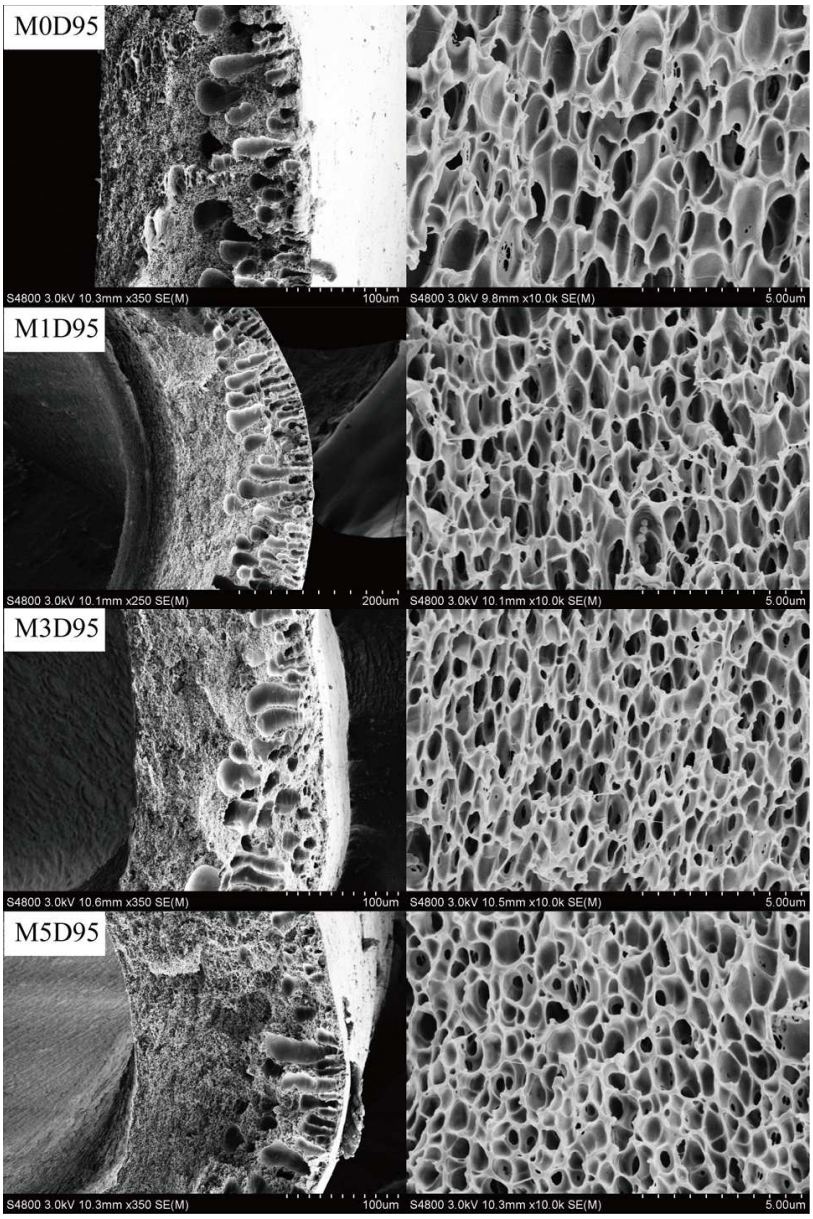

(B)

Fig.3 The cross-sectional FESEM images of PVC hollow fiber membranes (A) The bore fluid is 50 wt. % ethanol aqueous solution (B) The bore fluid is 95 wt.% DMAc aqueous solution

Table 2 Solubility parameters of PVC, solvents and bore liquids[4,40]

	δ_d/Mpa$^{1/2}$	δ_p/Mpa$^{1/2}$	δ_h/Mpa$^{1/2}$	δ/Mpa$^{1/2}$	$\delta_{s\text{-}p}$/Mpa$^{1/2}$

PVC	18.7	10.0	3.1	21.5	/
H_2O	15.5	16.0	42.4	47.9	40.3
DMAc	16.8	11.5	10.2	22.7	8.2
Ethanol	15.8	8.8	19.4	26.6	17.4
Ethanol:H_2O=50:50	15.7	12.0	29.5	35.5	27.2
DMAc:H_2O=95:5	16.7	11.7	11.7	23.9	9.6

Fig.3 shows the cross-sectional FESEM images of the PVC hollow fiber membranes. When 50 wt.% ethanol aqueous solution is used as bore liquid, the PVC membranes show double finger-like structure accompanied with sponge-like structure sandwiched in-between. This structure indicates that phase separation is induced by non-solvent penetrated from both inner and outer surfaces of hollow fiber membranes[42]. Meanwhile, the finger-like pores are suppressed and the sandwiched sponge-like structure of the fibers gradually grows with the addition of TEOS. For the membranes prepared from 95 wt.% DMAc aqueous solution as bore liquid, the single finger-like structure accompanied with major sponge-like structure is found for the fibers of M0(1,3,5)D95. Similarly, the sponge-like structure is gradually enhanced. The size and amount of finger-like pore decrease with the addition of TEOS. From Table.1, the dope viscosity increases with the addition of TEOS. The higher dope viscosity restricts the mass exchange rate between solvent and non-solvent, and slows down the demixing rate. Therefore, the sponge-like structure becomes thicker gradually for the two series of membranes. To explain the effect of bore liquid on membrane structure, the solubility parameter differences between solvent, non-solvent and bore liquid are calculated and showed in Table 2[40,43]. It can be seen that $\delta_{s\text{-}p}$ of water, 50 wt. % ethanol aqueous solution and 95 wt.% DMAc aqueous solution between polymer PVC are 40.3 $Mpa^{1/2}$, 27.2 $Mpa^{1/2}$ and 9.6 $Mpa^{1/2}$ respectively. The bigger $\delta_{s\text{-}p}$ value means faster demixing rate. In general, a delayed phase separation forms the membrane with a sponge-like

structure; while an instantaneous phase separation results in the membrane with a finger-like structure[34]. Therefore, the two bore fluids lead to the different structure of PVC hollow fiber membranes in Fig.3. According to the enlarged images of the sandwiched sponge-like structure, all membranes show porous structure which may be ascribed to the pore-forming effect of glycerol[44,45].

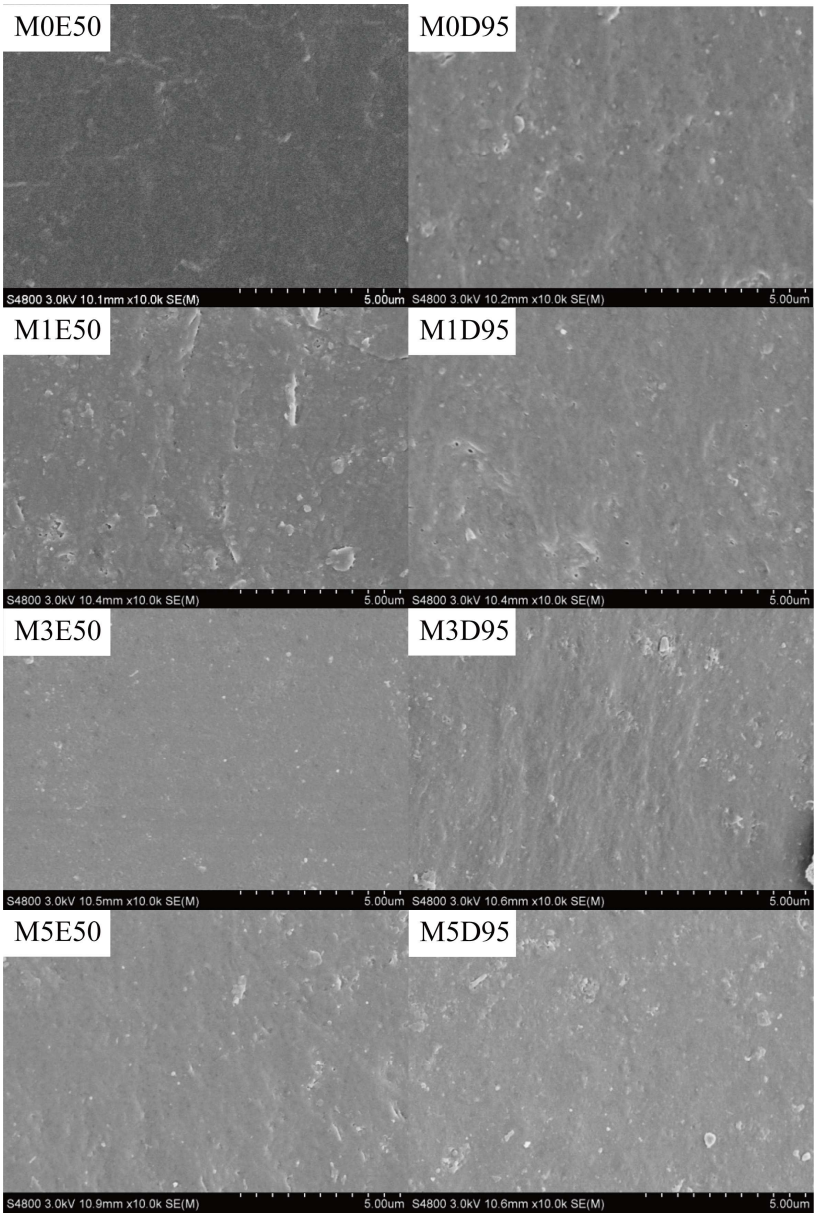

Fig.4 The outer FESEM images of PVC hollow fiber membranes.

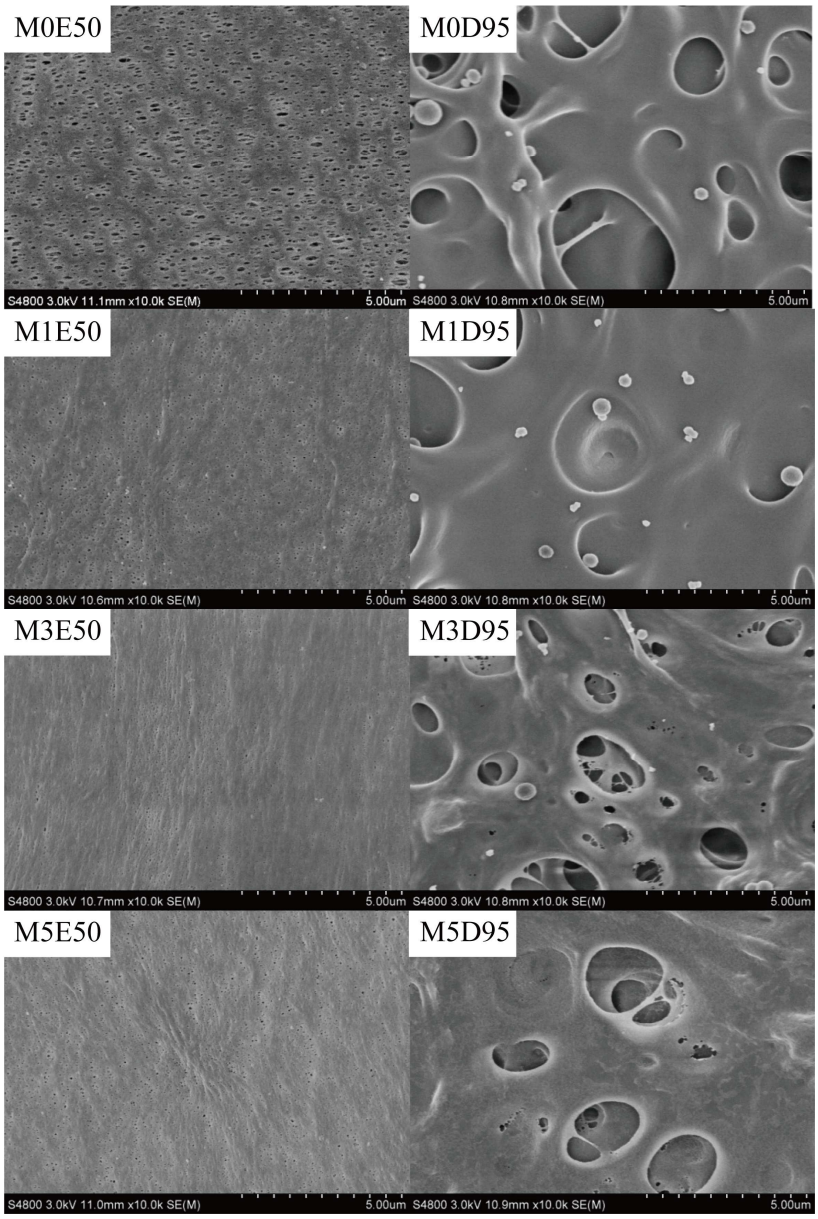

Fig.5 The inner FESEM images of PVC hollow fiber membranes

Fig.4 shows the FESEM images of the outer surfaces of PVC hollow fiber membranes. All membranes exhibit dense outer surfaces for water acting as a strong non-solvent. However, from Fig.5, it can be easily seen that two different bore liquids lead to different inner surfaces. Compared with the membranes M0(1,3,5)E50 prepared with 50 wt. % ethanol aqueous solution, the membranes M0(1,3,5)D95 fabricated with 95 wt.% DMAc aqueous solution as bore liquid show bigger pores. Also, the pore size of the inner surfaces may slightly decrease with the addition of TEOS due to the viscosity increasing of dopes.

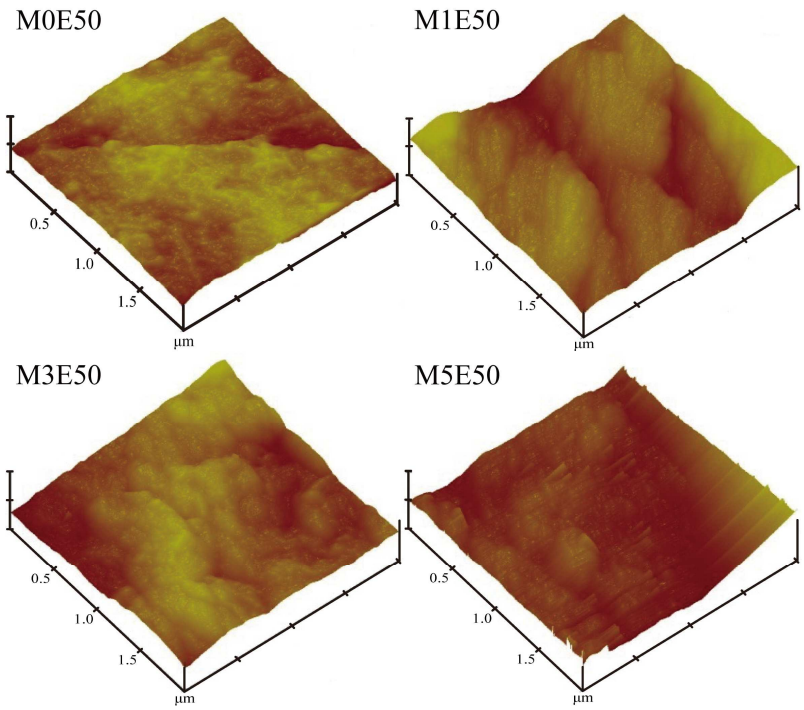

Fig.6. The AFM images of the outer surfaces of PVC hollow fiber membranes

Table 3 The AFM results of PVC hollow fiber membranes.

Membrane no.	R_a (nm)	R_q(nm)	R_{sk}	R_{ku}
M0E50	11.37	12.72	-0.43	2.42
M1E50	24.08	16.32	-0.72	4.78
M3E50	19.23	16.09	-0.26	2.97
M5E50	16.27	15.21	0.94	4.37

The outer surfaces of PVC hollow fiber membranes with 50 wt. % ethanol aqueous solution as bore liquid are also detected by AFM technique with tapping mode. The images and roughness parameters are illustrated in Fig.6 and Table 3. From Table 3, the membranes prepared with TEOS show higher surface roughness than that of pristine PVC membrane(M0E50), which can be ascribed to the relaxation of the orientated macromolecules with low dope viscosity [40]. Yan[46] *et al.* and Yu[30] *et al.* pointed out that higher roughness

commonly led to two changes in the modified membrane: an increase of efficient filtration area and a decrease of the anti-fouling performance. The larger filtration area is beneficial to water flux, which will be further discussed below. For numerous "valleys" on membrane surface, foulants tend to accumulate in them which result in flux decline and membrane fouling.

The negative R_{sk} for M0E50, M1E50 and M3E50 means that valleys dominate their surfaces and the positive value for M5E50 indicates peaks dominate its outer surface. According R_{ku} values, it can be seen that the introduction of silica results in uneven and nonrepetitive distribution for the outer surfaces.

3.3. Dynamic contact angle

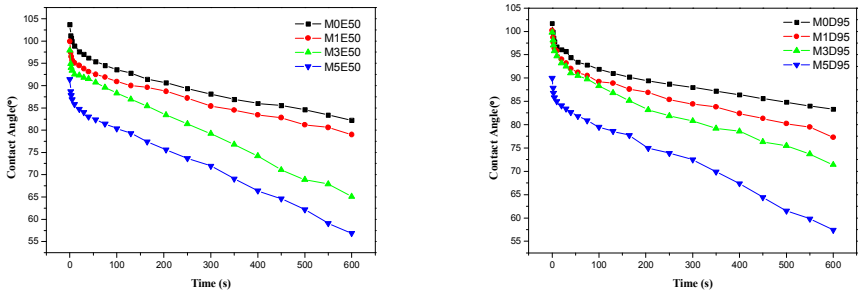

(A) (B)

Fig.7 The dynamic contact angles of PVC hollow fiber membranes (A) M0(1,3,5)E50 (B) M0(1,3,5)D95

Table 4 The final contact angles of PVC hollow fiber membranes

Membrane no.	Final contact angle(°)	Membrane no.	Final contact angle(°)
M0E50	82.2	M0D95	83.3
M1E50	79.0	M1D95	77.3
M3E50	65.1	M3D95	71.4
M5E50	56.9	M5D95	57.4

Commonly, the surface hydrophilcity of polymeric membranes is highly related to the permeation performance and anti-fouling ability. For PVC polymer, there is no hydrophilic chemical groups

on its structure which may lead to flux reduction and operation cost increase[6]. The dynamic contact angles of the PVC hollow fiber membranes as a function of time and the final contact angle data after 10 min are illustrated in Fig.7 and Table 4, respectively. It can be seen that the contact angles show an overall decrease tendency as the increase of TEOS concentration for the two series of membranes (M0(1,3,5)E50 and M0(1,3,5)D95).The final contact angles decrease from 82.2° to 56.9° for membranes M0(1,3,5)E50 with the TEOS concentration from 0 to 5 wt.% in dopes. Similarly, the contact angle decrease from 83.3° to 57.4° for M0(1,3,5)D95. This phenomenon should be attributed to the good hydrophilicity of silica generated by the hydrolysis and polycondensaton reaction of TEOS. The good membrane hydrophilicity results in good wetting and high water permeability. These results are similar to the previous publications[47-49]. Therefore, it verifies that the introduction of silica with a weak in situ sol-gel method can significantly improve the hydrophilicity of PVC membranes. Meanwhile, there is no big difference between the contact angles of membranes M0(1,3,5)E50 and those of membranes M0(1,3,5)D95 with the same dope composition.

3.4. Permeation and rejection performances

The hydraulic permeability (J_w), the calculated mean pore size ($\overline{d}_p$) and MWCO of the fabricated PVC hollow fiber membranes are shown in Table.5 and Fig.8. The results illustrate that J_w increases from 34.8 $L \cdot M^{-2} \cdot H^{-1} \cdot bar^{-1}$ to 48.7 $L \cdot M^{-2} \cdot H^{-1} \cdot bar^{-1}$ and 89.1 $L \cdot M^{-2} \cdot H^{-1} \cdot bar^{-1}$, and then decreases to 45.3 $L \cdot M^{-2} \cdot H^{-1} \cdot bar^{-1}$ for the membranes of M0(1,3,5)E50. The similar J_w variation tendency is found from 32.7 $L \cdot M^{-2} \cdot H^{-1} \cdot bar^{-1}$ to 43.6 $L \cdot M^{-2} \cdot H^{-1} \cdot bar^{-1}$ and 60.7 $L \cdot M^{-2} \cdot H^{-1} \cdot bar^{-1}$, and then decreases to 38.8 $L \cdot M^{-2} \cdot H^{-1} \cdot bar^{-1}$ for the membranes of M0(1,3,5)D95. As we known, the permeation performances are closely related to the porosity, interconnection of cavities, surface pore size and surface hydrophilicity of the membranes[18]. The hydrophilicity of the membranes increases with the increase of TEOS, which commonly results in higher water flux. However, the membranes with higher TEOS concentration in dopes exhibit thicker sponge-like structure with higher

permeation resistance and suppress the permeability [50]. The two contradictory factors determine the final permeation flux. For the two serials of PVC membranes, the surface hydrophilicity increasing dominants the permeabilities of the former three fibers M0(1,3)E50 and M0(1,3)D95; while the increased permeation resistance dominants the permeabilities of the fibers of M5E50 or M5D95.

Fig.8 and Table.5 illustrate that the MWCO and $\overline{d}_p$ values of the PVC hollow fiber membranes. For the membranes of M0(1,3,5)E50, the $\overline{d}_p$ decreases from 2.80 nm to 1.52 nm, and then increases to 2.04 nm. And the MWCO decreases from 55.9 KDa to 36.5 KDa and then increases to 42.9 KDa. The membranes of M0(1,3,5)D95 show similar tendency, whose $\overline{d}_p$ decreases from 3.18 nm to 2.67 nm and then increases to 3.01 nm. The MWCO decreases from 61.1 KDa to 42.2 KDa, and then increases to 48.4 KDa. Correlating the variation of J_w, $\overline{d}_p$ and MWCO values, it can be concluded that the hydraulic permeability of membranes is determined by not only the pore size but also the presence of silica on membranes surface.

Table 5 The hydraulic permeability, pore size and MWCO of PVC hollow fiber membranes

Membrane no.	J_w ($L \cdot M^{-2} \cdot H^{-1} \cdot bar^{-1}$)	$\overline{d}_p$ (nm)	MWCO (kDa)
M0E50	34.8±1.6	2.80	55.9
M0D95	32.7±2.0	3.18	61.1
M1E50	48.7±1.4	1.76	49.2
M1D95	43.6±0.9	3.18	50.8
M3E50	89.1±2.2	1.52	36.5
M3D95	60.7±1.9	2.67	42.2
M5E50	45.3±1.2	2.04	42.9
M5D95	38.8±1.8	3.01	48.4

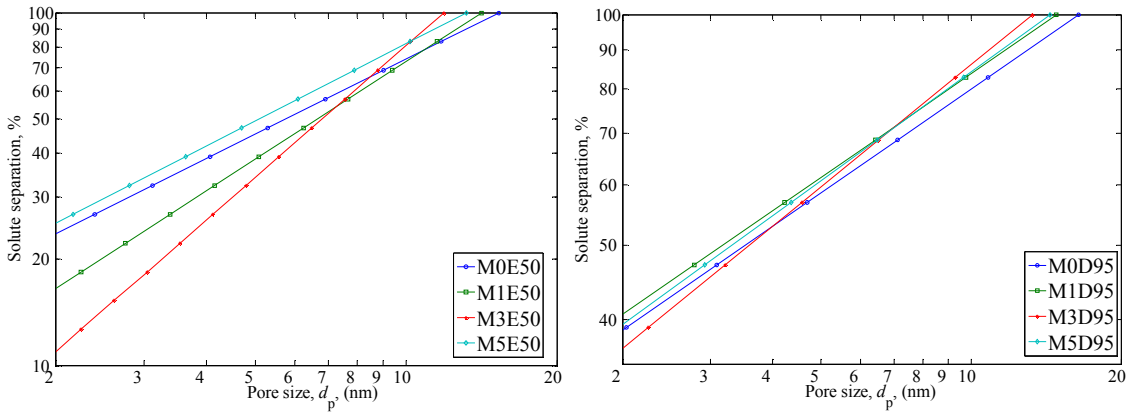

(A)

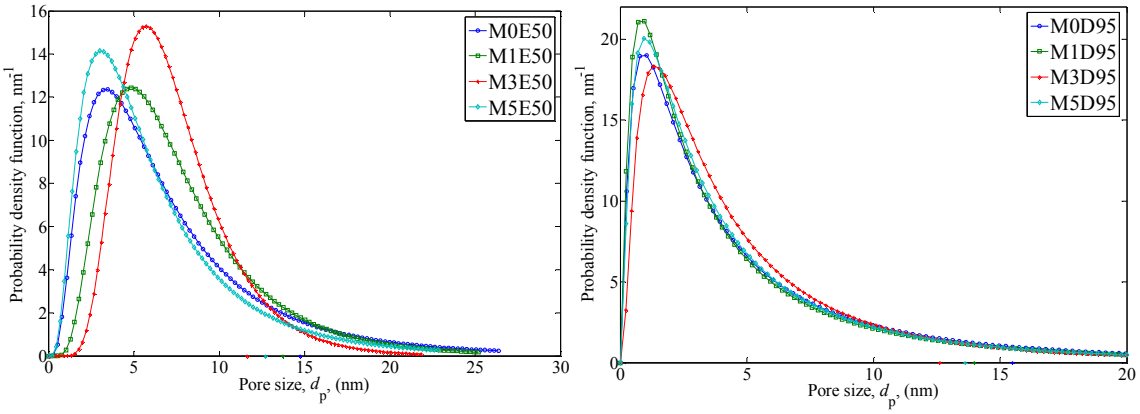

(B)

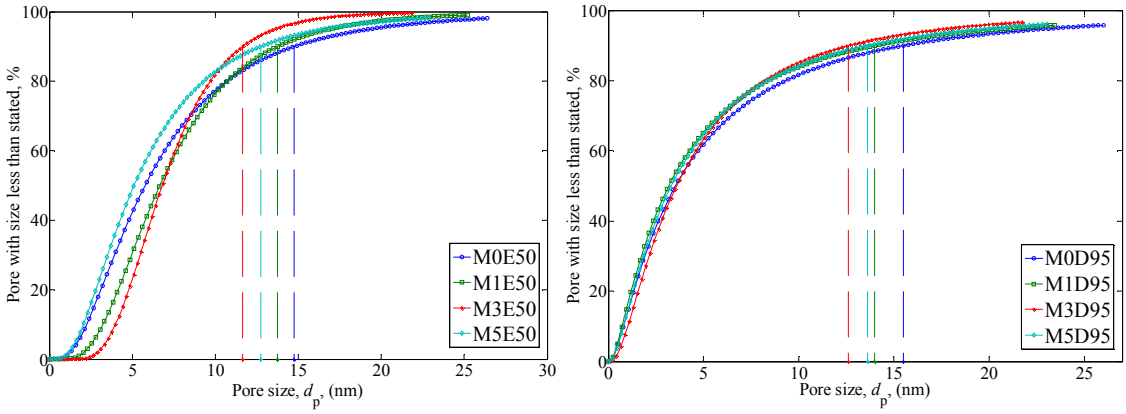

(C)

Fig.8 (A) Solute PEG rejection curves (B) probability density function curves (C) cumulative pore size

distribution curves of PVC hollow fiber membranes.

3.5. Anti-fouling performances

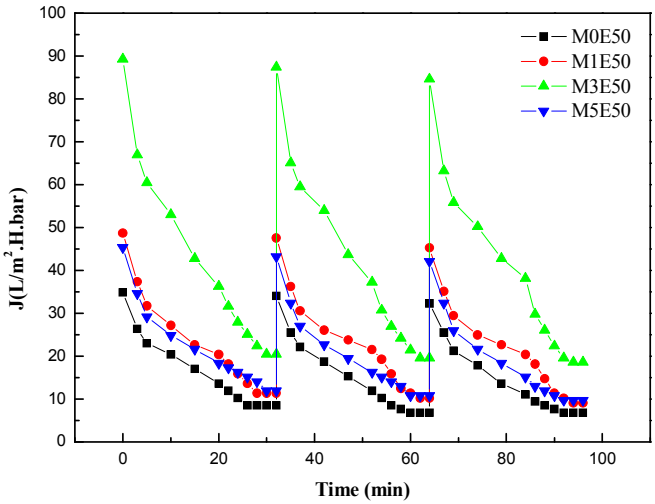

Fig.9 Anti-fouling experiments of PVC hollow fiber membranes

Table 6 The Anti-fouling parameters of PVC hollow fiber membranes

Membrane no.	FRR1 %	R_{J1} %	FRR2 %	R_{J2} %	FRR3 %
M0E50	75.6	97.6	79.9	95.0	80.0
M1E50	76.7	97.7	78.6	95.2	80.0
M3E50	77.1	97.9	77.7	96.8	78.0
M5E50	73.8	97.5	75.0	95.2	76.9

As we known, the permeation flux often significantly decreases during separation process due to membrane fouling[51]. The anti-fouling properties of M0(1,3,5)E50 are illustrated in Fig.9 and Table 6. From Fig.9, it can be seen that the permeation flux significantly decreases when deionized water was replaced by

BSA aqueous solution for membrane fouling and concentration polarization. However, after washing with NaClO aqueous solution, the permeation fluxes of the four PVC hollow fiber membranes are well recovered. The recovery rates of four membranes in two washing cycles are both higher than 95.0 %, which indicates that the fouled membranes are easily regenerated by the washing process. Additionally, the fiber of M3E50 has the highest permeation flux for BSA aqueous solution, which is markedly higher than those of other fibers. It verifies that introducing appropriate silica with a weak in situ sol-gel method is an effective method to modify PVC ultrafiltration membranes.

3.6. The mechanical properties of the PVC hollow fiber membranes

The break strain, elongation at break and Young's modulus of the PVC hollow fiber membranes are summered in Table7. It can be seen that for the two serials of PVC fibers with different bore liquids, the three indicators all increase with the addition of silica into the membranes. As 50 wt.% ethanol aqueous solution is used as bore liquid, the break strain values of the membranes M0(1,3,5)E50 increase from 1.53±0.16 MPa to 3.76±0.07 MPa, the elongation ratio increases from 56.3±2.1% to 70.8±6.2 %, and the Young modulus increases from 49.4±3.7 MPa to 91.9±4.4 MPa with the addition of TEOS from 0 to 5 wt.% in dopes. The similar trend is found for the membranes M0(1,3,5)D95 with 95 wt.% aqueous solution as bore liquid. The increased mechanical strength of PVC fibers should be ascribed to two factors: the variation of membrane morphology and the introduced silica. The images of the cross sections of PVC fibers illustrate that the sponge-like structure grows with the addition of TEOS, which is advantageous to the improvement of mechanical properties. Also, the introduced inorganic silica by weak in situ sol-gel method also promotes the improvement of mechanical properties of the fibers. Additonlly, from Table 7, it also can be seen that the fibers of M0(1,3,5)E50 have lower mechanical properties than those of M0(1,3,5)D95 with the same dope. It also attributed to the morphology difference between the two serials of fibers.

Table 7 The mechanical properties of the PVC hollow fiber membranes.

Membrane no.	Break strain (MPa)	Elongation at break (%)	Young's modulus (MPa)
M0E50	1.53±0.16	56.3±2.1	49.4±3.7
M0D95	2.12±0.17	66.7±6.3	56.8±5.9
M1E50	1.91±0.10	61.5±5.4	53.7±2.4
M1D95	2.60±0.18	68.9±4.7	76.0±3.3
M3E50	2.81±0.46	63.7±4.3	84.0±5.9
M3D95	2.90±0.17	71.1±4.2	77.0±4.3
M5E50	3.76±0.07	70.8±6.2	91.9±4.4
M5D95	3.20±0.19	80.2±3.3	86.6±4.6

4. Conclusions

A weak in situ sol-gel method is successfully employed to modify PVC hollow fiber membranes with silica by the soft hydrolysis reaction of TEOS in water, which avoids using corrosive substances during membrane preparation. The effects of TEOS concentration and bore liquids on membrane morphologies, hydrophilicity, permeability, anti-fouling ability, pore size and mechanical properties are discussed in detail. The FESEM images show that the sponge-like structure of PVC hollow fibers expands and the finger-like structure is suppressed with the addition of TEOS in the dopes. The introduced silica is uniformly distributed on membrane surface, which significantly improves the membrane hydrophilicity and permeability. The highest J_w value of 89.3 $L \cdot M^{-2} \cdot H^{-1} \cdot bar^{-1}$ is obtained. The mechanical strength of PVC fibers is also gradually enhanced with the addition TEOS.

Acknowledgments

The research is supported by Science and Technology Commission of Shanghai Municipality

(13ZR1429900, 14520502900) and Internation Joint Laboratory on Resource Chemistry (IJLRC).

Nomenclature

J_w The pure water flux ($L \cdot M^{-2} \cdot H^{-1} \cdot bar^{-1}$)

V Volume of penetrative water (L)

A The effective permeation area of membrane (m^2)

t The time of getting the received pure water (h)

ΔP The penetrative pressure difference (bar)

RFR Relative flux reduction(%)

R_J The flux recovery ratio (%)

J_p BSA aqueous solution flux after each fouling process ($L \cdot M^{-2} \cdot H^{-1} \cdot bar^{-1}$)

J_R The re-measured water flux of the membranes in each cycle. ($L \cdot M^{-2} \cdot H^{-1} \cdot bar^{-1}$)

R The Stokes radius of the solutes (m)

M The molecular weight ($kg \cdot mol^{-1}$)

References

[1] J.-M. Yang, N.-C. Wang and H.-C. Chiu, J.Membr.Sci., 2014, 457, 139-148.

[2] C. Zhou, Y. Gao, X. Qi, Z. Tan, S. Sun and H. Zhang, J. Vinyl. Addit. Techn., 2013, 19, 11-17.

[3] C.-X. Liu, W.-Z. Lang, B.-B. Shi and Y.-J. Guo, Mater. Lett., 2013, 107, 53-55.

[4] Q.F. Alsalhy, Desalination, 2012, 294, 44-52.

[5] N. Misra, H.S. Panda, G. Kapusetti, S. Jaiswal, S.C. Gopal and U.S. Sharma, J. Polym. Mater., 2011, 28, 139-148.

[6] S. Mei, C. Xiao, X. Hu and W. Shu, Desalination, 2011, 280, 378-383.

[7] S. Mei, C. Xiao and X. Hu, J. Appl. Polym. Sci., 2011, 120, 557-562.

[8] W. Ma, H. Otsuka and A. Takahara, Polymer, 2011, 52, 5543-5550.

[9] Q.-r. Fan, P. Xiao, F. Xiao, C.-g. Qiao, T. Qin and D.-s. Wang, Environ. Sci.-China, 2011, 32, 1351-1356.

[10] Q. Alsalhy, S. Algebory, G.M. Alwan, S. Simone, A. Figoli and E. Drioli, Separ. Sci. Technol., 2011, 46, 2199-2210.

[11] X. Zhang, Y. Chen, A.H. Konsowa, X. Zhu and J.C. Crittenden, Sep. Purif. Technol., 2009, 70, 71-78.

[12] M. Khayet, M.C. García-Payo, F.A. Qusay and M.A. Zubaidy, J.Membr.Sci., 2009, 330, 30-39.

[13] X. Guo, Q. Li, W. Hu, W. Gao and D. Liu, J.Membr.Sci., 2009, 327, 254-263.

[14] F. Liu, N.A. Hashim, Y. Liu, M.R.M. Abed and K. Li, J. Membr. Sci., 2011, 375, 1-27.

[15] J.-H. Kim and K.-H. Lee, J. Membr. Sci., 1998, 138, 153-163.

[16] W.-Z. Lang, Q. Ji, J.-P. Shen, Y.-J. Guo and Z.-L. Xu, Desalination, 2012, 292, 45-52.

[17] W.-Z. Lang, X. Zhang, J.-P. Shen, H.-P. Xu, Z.-L. Xu and Y.-J. Guo, Desalination, 2014, 341, 72-82.

[18] H.-P. Xu, W.-Z. Lang, X. Yan, X. Zhang and Y.-J. Guo, J.Membr.Sci., 2014, 467, 142-152.

[19] F. Shi, Y. Ma, J. Ma, P. Wang and W. Sun, J. Membr. Sci., 2013, 427, 259-269.

[20] J. Hong and Y. He, Desalination, 2014, 332, 67-75.

[21] A. Cui, Z. Liu, C. Xiao and Y. Zhang, J.Membr.Sci., 2010, 360, 259-264.

[22] X. Zuo, S. Yu, X. Xu, J. Xu, R. Bao and X. Yan, J.Membr.Sci., 2009, 340, 206-213.

[23] A. Cui, Z. Liu, C. Xiao and Y. Zhang, J. Membr. Sci., 2010, 360, 259-264.

[24] R. Ciriminna, A. Fidalgo, V. Pandarus, F. Béland, L.M. Ilharco and M. Pagliaro, Chem. Rev., 2013, 113, 6592-6620.

[25] H.-Q. Liang, Q.-Y. Wu, L.-S. Wan, X.-J. Huang and Z.-K. Xu, J.Membr.Sci., 2014, 465, 56-67.

[26] F. Zhang, W. Zhang, Y. Yu, B. Deng, J. Li and J. Jin, J. Membr. Sci., 2013, 432, 25-32.

[27] H.F. Qureshi, A. Nijmeijer and L. Winnubst, J.Membr.Sci., 2013, 446, 19-25.

[28] W. Chen, Y. Su, L. Zhang, Q. Shi, J. Peng and Z. Jiang, J.Membr.Sci., 2010, 348, 75-83.

[29] R.A. Zoppi and C.G.A. Soares, Adv. Polym. Tech., 2002, 21, 2-16.

[30] L.-Y. Yu, Z.-L. Xu, H.-M. Shen and H. Yang, J. Membr. Sci., 2009, 337, 257-265.

[31] X. Zhang, W.-Z. Lang, H.-P. Xu, X. Yan, Y.-J. Guo and L.-F. Chu, J.Membr.Sci., 2014.

[32] J. Stawikowska and A.G. Livingston, J.Membr.Sci., 2013, 425-426, 58-70.

[33] W.-Z. Lang, J.-P. Shen, Y.-X. Zhang, Y.-H. Yu, Y.-J. Guo and C.-X. Liu, J. Membr. Sci., 2013, 430, 1-10.

[34] W.-Z. Lang, Z.-L. Xu, H. Yang and W. Tong, J.Membr.Sci., 2007, 288, 123-131.

[35] Y. Zhang, J. Tian, H. Liang, J. Nan, Z. Chen and G. Li, J. Environ. Sci., 2011, 23, 529-536.

[36] X. Guo, H. Shao, W. Hu and H. Shen, Desalin.Water.Treat., 2011, 33, 231-239.

[37] M. Gholami, Simin Nasseri, C.Y. Feng, T. Matsuura and K.C. Khulbe, Desalination, 2003, 293-301.

[38] Q. Yang, T.-S. Chung and Y.E. Santoso, J.Membr.Sci., 2007, 290, 153-163.

[39] X. Zhang, W.-Z. Lang, H.-P. Xu, X. Yan, Y.-J. Guo and L.-F. Chu, J. Membr. Sci., 2014, 469, 458-470.

[40] W.-Z. Lang, J.-P. Shen, Y.-T. Wei, Q.-Y. Wu, J. Wang and Y.-J. Guo, Chem. Eng. J., 2013, 225, 25-33.

[41] J. Shirley, S. Mandale and V. Kochkodan, Desalination, 2014, 344, 116-122.

[42] Z. Yuan and X. Dan-Li, Desalination, 2008, 223, 438-447.

[43] Z.-L. Xu and F. Alsalhy Qusay, J.Membr.Sci., 2004, 233, 101-111.

[44] L. Shi, R. Wang, Y. Cao, D.T. Liang and J.H. Tay, J. Membr. Sci., 2008, 315, 195-204.

[45] M.A. Aroon, A.F. Ismail, M.M. Montazer-Rahmati and T. Matsuura, Sep. Purif. Technol., 2010, 72, 194-202.

[46] L. Yan, Y. Li, C. Xiang and S. Xianda, J. Membr. Sci., 2006, 276, 162-167.

[47] G. Arthanareeswaran, T. Sriyamunadevi and M. Raajenthiren, Sep. Purif. Technol., 2008, 64, 38-47.

[48] J. Huang, K.S. Zhang, K. Wang, Z.L. Xie, B. Ladewig and H.T. Wang, J.Membr.Sci., 2012, 423, 362-370.

[49] Z.J. Yu, X.Y. Liu, F.B. Zhao, X.Y. Liang and Y. Tian, J. Appl. Polym. Sci., 2015, 132.

[50] L. García-Fernández, M.C. García-Payo and M. Khayet, J. Membr. Sci., 2014, 468, 324-338.

[51] S. Zinadini, A.A. Zinatizadeh, M. Rahimi, V. Vatanpour and H. Zangeneh, J. Membr. Sci., 2014, 453, 292-301.

Table captions

Table.1 The detailed preparation conditions of PVC hollow fiber membranes

Table.2 Solubility parameters of PVC, solvents and bore liquids

Table.3 The AFM results of PVC hollow fiber membranes

Table.4 The final contact angles of PVC hollow fiber membranes

Table.5 The hydraulic permeability, pore size and molecular weight cut-off (MWCO) of PVC hollow fiber membranes

Table.6 The Anti-fouling parameters of PVC hollow fiber membranes

Table.7 The mechanical properties of the PVC hollow fiber membranes

Figure captions

Fig.1 The FTIR-ATR spectra of membrane M5E50

Fig.2 The EDS maps of membrane M5E50

Fig.3 The cross-sectional FESEM images of PVC hollow fiber membranes

Fig.4 The outer FESEM images of PVC hollow fiber membranes

Fig.5 The inner FESEM images of PVC hollow fiber membranes

Fig.6 The AFM images of the outer surfaces of PVC hollow fiber membranes

Fig.7 The dynamic contact angles of PVC hollow fiber membranes (A) M0(1,3,5)E50 (B) M0(1,3,5)D95

Fig.8 (A) Solute PEG rejection curves (B) probability density function curves (C) cumulative pore size distribution curves of PVC hollow fiber membranes (1) M0(1,3,5)E50 (2) M0(1,3,5)D95

Fig.9 Anti-fouling experiments of PVC hollow fiber membranes